Preprints of the 19th World Congress
The International Federation of Automatic Control
Cape Town, South Africa. August 24-29, 2014

Vector Field Guided Auto-Landing Control of Airship with Wind Disturbance

Ji-Wook Kwon[1]. Jin Hyo Kim[1,2]. Jiwon Seo[1,2]

[1]*Yonsei Institute of Convergence Technology, Yonsei University, Incheon 406-840, Korea*
[2]*School of Integrated Technology, Yonsei University, Incheon 406-840, Korea*
(Tel: 82-32-749-5833; bluemichael, jinhyo.kim, and jiwon.seo@yonsei.ac.kr).

Abstract: This paper proposes a vector field guided auto-landing control of an airship with a wind disturbance, whose motion is described in a vertical plane. Whereas hovering and vertical landing abilities are advantages of the airship, there is little research on the auto-landing mechanism. Unlike the previous airship control algorithms which compensate the disturbances using linear and nonlinear control laws such as backstepping control methods, the proposed auto-landing control algorithm is simpler than the backstepping controllers and covers the wind disturbances with unknown bound. To this end, the vector field based guidance law achieving the control objectives and adaptive-robust dynamic control law realizing the desired course are proposed. The stability analysis and simulation results of the proposed auto-landing control law are included to demonstrate the practical applicability of the proposed method.

Keywords: airship control, auto-landing control, vector field based guidance law, adaptive-robust control

1. INTRODUCTION

Airship has become an interesting type of an unmanned aerial vehicle (UAV) for past few years because of a reappraisal of contributions of the airship. The airship has been employed to various applications such as indoor and outdoor advertising tasks, a fire detection, an inspection of big structures, a surveillance of a borderline, and military applications since the airship can hover for a long time, consume little energy, take-off and land vertically, and have large payload (Pavia et al., 2006; Solaque et al., 2008; Azinheira et al., 2008). Also, these advantages have derived developments of the following actual airship in real environment: AURORA, High-Altitude Airship of Lockheed Martine, Stratospheric Airship, etc. (Zheng et al., 2012). Particularly, the hovering ability among the contributions of the airship has been researched (Pavia et al., 2006; Azinheira et al., 2008), which can provide the applications such as manipulation of big objects or the surveillance of local area. These applications do not require only the hovering ability, but also, vertical landing. That is, it can improve the performance of the airship to land automatically while keeping the position over the landing point.

To control the airship, there were PID control (Kahale et al., 2013) and dynamic inversion (Moutinho et al., 2005) algorithms which can be implemented in a simple way. However, these methods could not compensate the wind disturbances. To control the airship with the wind disturbances in real environments, backstepping control algorithms which compensate the wind disturbances were proposed (Kahale et al., 2013; Azinheira et al., 2008). These nonlinear control algorithms improve the performances of the airship with the model uncertainties and the disturbances under the path-following task in flight phase. Also, the input constraint of the airship was considered (Azinheira et al., 2008). However, in the previous work regarding the wind disturbances, it was assumed that the bound of the disturbance is known (Kahale et al., 2013), and the backstepping control mechanism is still complicated (Chaw, 2010). In addition, there is little research on the auto-landing control of the airship. There is a lack of sufficient generality for a flight phase as a landing phase is because of the ground effect of the airship in the vicinity of the ground (Malaek et al., 2004).

Thus, this paper proposes the vector field guided auto-landing control algorithm for the airship in the landing phase with the wind disturbance. To this end, it is assumed that longitudinal and lateral motions can be departed (Pavia et al., 2006), the simplified model of airship is employed (Solaque et al., 2008), and the airship can face the goal position using the control algorithms proposed in the previous works regarding the motion of the airship in the horizontal plane (Zheng et al., 2012; Pavia et al., 2006; Azinheira et al., 2008). From these assumptions, the airship is re-described in vertical plane with respect to the airship position and the goal position. To provide the approaching course toward the goal position, the vector field based guidance law is introduced, and then, the desired direction and the velocities of the airship generated by the proposed guidance law are realized by an adaptive robust velocity control algorithm using the modified trajectory tracking control algorithm proposed in Chaw (2010), such that the wind disturbances are compensated while regarding the input constraints. Therefore, the proposed auto-landing control algorithm provides the following advantages to the airship: 1) the control algorithm is simple than the previous backstepping control mechanism; 2) the wind disturbance with the unknown bound are compensated; and 3) the airship is controlled despite of the

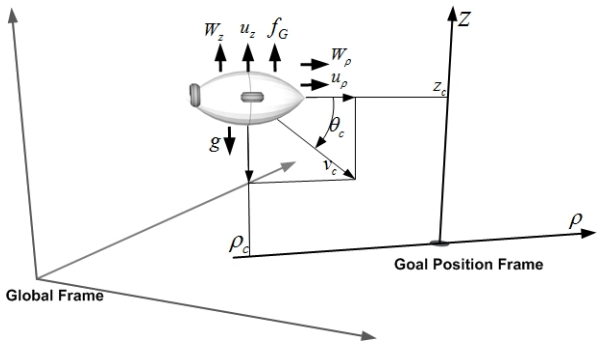

Fig. 1. The projected simplified model of the airship in the vertical plane.

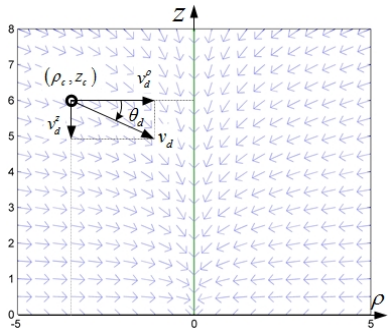

Fig. 2.The guidance law based on the vector field.

limited inputs. This paper is organized as follows. We show the decoupled airship model in Section 2, and we introduce the novel vector field for the auto-landing method in Section 3. In Section 4, the desired velocity generation and the velocity control law are proposed. To demonstrate the usefulness of the proposed control algorithm, simulation results are presented in Section 5. Finally, the conclusions of the study are given in Section 6.

2. AIRSHIP MODEL

This paper considers the two dimensional vertical movement of the airship, where longitudinal and vertical motions are included. For these projected motion, it is assumed that the airship can face the goal position using the already suggested yaw angle controls on the horizontal plane. The motion of the airship on the vertical plane is depicted in Fig. 1.

In Fig. 1, (ρ_c, z_c) is current position of the airship in the goal position frame, θ_c is the moving direction, f_G is the upstream force from the gas in the airship, g is the gravity force, v_c is the velocity of the airship, (v_ρ, v_z) are the velocities along each axis, and (W_ρ, W_z) is the wind disturbances which are bounded as $|W_\rho| \le D_\rho$ and $|W_z| \le D_z$ where D_ρ and D_z are unknown. It is possible that the airship in Fig. 1 is described as the following decoupled and simplified model:

$$M\ddot{\rho}_c = u_\rho + W_\rho \tag{1 a}$$

$$M\ddot{z}_c = u_z + f_G - g + W_z \tag{1 b}$$

where M is a mass of the airship, u_ρ and u_z are control inputs. Also, the relationships of θ_c, v_c, v_ρ, and v_z are represented as

$$\dot{\rho}_c = v_c \cos\theta_c \tag{2 a}$$

$$\dot{z}_c = v_c \sin\theta_c \tag{2 b}$$

$$\theta_c = \text{atan2}(v_z, v_\rho) \tag{2 c}$$

where atan2(·) is a four-quadrant invers tangent determined in the intervals (-π, π].

3. VECTOR FIELD BASED GUIDANCE LAW

This section shows the guidance law based on the vector field where the airship is guided toward the goal position. The vector field with respect to the goal position is presented in Fig. 2. Fig. 2 shows the desired course on the two-dimensional vertical plane. The desired course toward the goal position is presented as the arrows which are the direction of the vector field. v_d is the desired velocity (v_d will be designed in the following section), (v_d^ρ, v_d^z) are the projected desired velocities on each axis, which are acquired as

$$v_d^\rho = v_d \cos\theta_d \tag{3 a}$$

$$v_d^z = v_d \sin\theta_d, \tag{3 b}$$

and θ_d is the desired moving direction determining the approaching angle to the goal position, which is the direction of the arrows in Fig. 2. On the vertical plane, the airship is guided to the goal position by the desired direction designed as follows.

$$\theta_d(\rho_c, z_c) = -\frac{\pi}{2} - \tan^{-1}\left(\frac{k_d \rho_c}{z_c}\right) \tag{4}$$

where k_d is positive constant which influences the transition rate of the vector field. If ρ_c goes to $-\infty$ or ∞, then θ_d converges to 0 or $-\pi$, respectively, and if ρ_c goes to 0, then θ_d converges to $-\pi/2$. Also, unlike the vector field based motion control on the horizontal plane, in the proposed auto-landing algorithm, the desired moving direction θ_d is designed using not only the ground distance, ρ_c, between the airship and the goal position, but also, the altitude of the airship, z_c, because the desired course for the landing process should consider the collision with the ground. If z_c becomes small, then the change rate of θ_d becomes small too, also, if z_c becomes 0, then θ_d does not change at all.

Remark: since k_d in (4) determines the transition rate of the desired moving direction along the ground distance between the airship and the goal position. This influence of k_d is represented in Fig. 3. As can be seen in Fig. 3, if k_d is small value, desired direction determined toward the goal position,

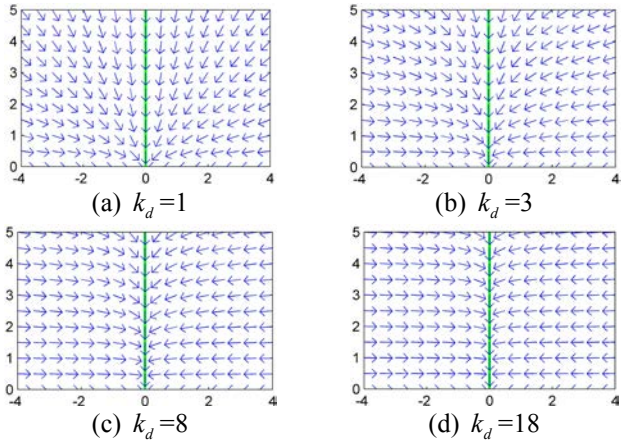

(a) k_d=1 (b) k_d=3

(c) k_d=8 (d) k_d=18

Fig. 3. The effect of k_d to the vector field.

and if k_d becomes bigger value, the direction of the vector field is changed rapidly around the z-axis. Therefore, the various change rate of the desired course with respect to the altitude and the ground distance between airship and the goal position is allowed because of the proposed vector field in (4). Indeed, it should be shown that the airship goes to the goal position when it moves along the desired coursed generated in (4). To this feasibility of the proposed desired moving direction, the following lemmas show the convergence of the errors (Kingston and Beard, 2007).

Lemma 1 (Ground distance convergence): The ground distance between the airship and the goal position converges to zero if the airship follows θ_d.

Proof: To show the convergence of the ρ_c to zero, we define θ_d^* as

$$-\frac{\pi}{2} \le \theta_d^* = \theta_d - \left(-\frac{\pi}{2}\right) \le \frac{\pi}{2}. \tag{5}$$

Then the time derivative of ρ_c becomes

$$\begin{aligned} \dot{\rho}_c &= v_d \cos\theta_d = v_d \cos\left(\theta_d^* + \frac{\pi}{2}\right) \\ &= v_d \sin\theta_d^*. \end{aligned} \tag{6}$$

When the sign of ρ_c and θ_d^* are compared using (5) and (6),

$$\begin{aligned} &\operatorname{sgn}\left(-\theta_d^*\right) = \operatorname{sgn}\left(\rho_c\right) \\ &\Rightarrow \operatorname{sgn}\left(-v_d \sin\theta_d^*\right) = \operatorname{sgn}\left(\rho_c\right) \\ &\Rightarrow \operatorname{sgn}\left(-\dot{\rho}_c\right) = \operatorname{sgn}\left(\rho_c\right) \\ &\Rightarrow \dot{\rho}_c \rho_c \le 0. \end{aligned} \tag{7}$$

Lyapunov function $V_\rho = \rho_c^2/2$ is chosen, whose time derivative is negative definite as $\dot{V}_\rho = \dot{\rho}_c \rho_c \le 0$, $\rho_c \to 0$ as $t \to \infty$ (Khalil, 1992). (Q.E.D.)

Lemma 2 (Altitude convergence): The altitude of the airship converges to zero if the proposed landing algorithm is employed to the airship in the landing phase.

Proof: When θ_d^* in Lemma 1 is used, the time derivative of z_c becomes

$$\begin{aligned} \dot{z}_c &= v_d \sin\theta_d = v_d \sin\left(\theta_d^* + \frac{\pi}{2}\right) \\ &= -v_d \cos\theta_d^*. \end{aligned} \tag{8}$$

When the sign of z_c and θ_d^* are compared using (8), since

$$\begin{aligned} &\operatorname{sgn}\left(v_d \cos\theta_d^*\right) = \operatorname{sgn}\left(z_c\right) \\ &\Rightarrow \operatorname{sgn}\left(-v_d \cos\theta_d^*\right) = \operatorname{sgn}\left(-z_c\right) \\ &\Rightarrow \operatorname{sgn}\left(\dot{z}_c\right) = \operatorname{sgn}\left(-z_c\right) \\ &\Rightarrow \dot{z}_c z_c \le 0, \end{aligned} \tag{9}$$

Lyapunov function $V_z = z_c^2/2$ is chosen, whose time derivative is negative definite as $\dot{V}_z = \dot{z}_c z_c \le 0$, then it is possible to show that $z_c \to 0$ as $t \to \infty$ (Khalil, 1992). (Q.E.D.)

Accordingly, we can show that the airship in the landing phase converges to goal position if the airship follows the proposed desired course generated by the vector field.

4. DECOUPLED AIRSHIP CONTROL

The desired velocity and moving direction are realized by the proposed decoupled velocity control algorithm which makes the actual longitudinal and vertical velocities converge to the desired velocities, v_d^ρ and v_d^z. To this end, we design the desired velocity based on Chwa (2010) as follows:

$$v_d = -k_p \left\{ \tanh\left(\rho_c / k_p\right) \cos\theta_d + \tanh\left(z_c / k_p\right) \sin\theta_d \right\} \tag{10}$$

where k_p is the positive constant. The feasibility of the proposed desired velocity in (10) is stated in the following theorem.

Theorem 1(The desired velocity generation): Consider the dynamic model of the airship and the desired course achieved from the vector field in Figs. 1 and 2. If the desired velocity in (10) is employed to the airship, ρ_c and z_c converge to zero asymptotically as $t \to \infty$.

Proof: We showed that the airship converges to the goal position while the airship follows the proposed desired course from the vector field. This finding derives that the desired velocity can be designed with respect to the desired moving direction.

Subscribing the desired velocity to (2), then (2) becomes

$$\begin{bmatrix} \dot{\rho}_c \\ \dot{z}_c \end{bmatrix} = v_d \begin{bmatrix} \cos\theta_d \\ \sin\theta_d \end{bmatrix}. \tag{11}$$

If (11) becomes

$$\begin{bmatrix} \dot{\rho}_c \\ \dot{z}_c \end{bmatrix} = v_d \begin{bmatrix} \cos\theta_d \\ \sin\theta_d \end{bmatrix} = -k_p \begin{bmatrix} \tanh\left(\rho_c / k_p\right) \\ \tanh\left(z_c / k_p\right) \end{bmatrix}, \tag{12}$$

then ρ_c and z_c converge to zero as $t \to \infty$. To acquire the desired velocity, $\begin{bmatrix}\cos\theta_d & \sin\theta_d\end{bmatrix}$ is multiplied to both sides in (12). Then (12) becomes

$$\begin{bmatrix}\cos\theta_d & \sin\theta_d\end{bmatrix} v_d \begin{bmatrix}\cos\theta_d \\ \sin\theta_d\end{bmatrix} = -k_p \begin{bmatrix}\cos\theta_d & \sin\theta_d\end{bmatrix} \begin{bmatrix}\tanh\left(\rho_c / k_p\right) \\ \tanh\left(z_c / k_p\right)\end{bmatrix}$$

$$\left(\cos^2\theta_d + \sin^2\theta_d\right) v_d = -k_p \begin{bmatrix}\cos\theta_d & \sin\theta_d\end{bmatrix} \begin{bmatrix}\tanh\left(\rho_c / k_p\right) \\ \tanh\left(z_c / k_p\right)\end{bmatrix} \tag{13}$$

From (13), we can acquire the desired velocity as in (10).

(Q.E.D.)

The designed desired velocity can be realized by the velocity control laws which control the actual velocities in (2) to converge to the desired velocities in (3) and (10). To this end, we choose the following velocity errors.

$$e_v^\rho = v_d^\rho - \dot{\rho}_c \text{ and } e_v^z = v_d^z - \dot{z}_c \tag{14}$$

whose time derivatives are

$$\begin{aligned}\dot{e}_v^\rho &= \dot{v}_d^\rho - \ddot{\rho}_c \\ &= \dot{v}_d^\rho - \frac{1}{M}\left(u_\rho + W_\rho\right) \\ \dot{e}_v^z &= \dot{v}_d^z - \ddot{z}_c \\ &= \dot{v}_d^z - \frac{1}{M}\left(u_z + f_G - g + W_z\right).\end{aligned} \tag{15}$$

From (14)-(15), the velocity control laws are determined as

$$\begin{aligned}u_\rho &= M\left(\dot{v}_d^\rho + k_v \tanh\left(e_v^\rho / k_v\right)\right) + \hat{D}_\rho \operatorname{sgn}\left(e_v^\rho\right) \\ u_z &= M\left(\dot{v}_d^z + k_v \tanh\left(e_v^z / k_v\right)\right) + f_G - g + \hat{D}_z \operatorname{sgn}\left(e_v^z\right).\end{aligned} \tag{16}$$

where k_v is the positive constant and $\hat{D}_\rho$ and $\hat{D}_z$ are estimates of the known bounds of the wind disturbances, whose adaptive laws are as follows:

$$\begin{aligned}\dot{\hat{D}}_\rho &= \gamma_\rho \left|e_v^\rho\right| / M \\ \dot{\hat{D}}_z &= \gamma_z \left|e_v^z\right| / M\end{aligned} \tag{17}$$

where γ_ρ and γ_z are the positive constants. The stability of the proposed velocity control inputs in (16) and the adaptive laws in (17) are presented in the following theorem.

Theorem 2 (The velocity control laws): When the designed control law in (16) and the adaptive laws in (17) are substituted to the dynamics in (1), the velocity errors of the airship converge to zero as $t \to \infty$ and the estimates of the unknown bounds goes to the real values.

Proof: To show the convergence of e_v^ρ and e_v^z to zero and the convergence of $\hat{D}_\rho$ and $\hat{D}_z$ to the real values, the Lyapunov function candidate is chosen as

$$V = \left(\left(e_v^\rho\right)^2 + \left(e_v^z\right)^2\right)/2 + \tilde{D}_\rho^2 / \gamma_\rho + \tilde{D}_z^2 / \gamma_z \tag{18}$$

where $\tilde{D}_\rho = D_\rho - \hat{D}_\rho$ and $\tilde{D}_z = D_z - \hat{D}_z$ are estimation errors of bounds of wind disturbances. Then, the time derivative of V in (18) becomes

$$\begin{aligned}\dot{V} &= e_v^\rho \dot{e}_v^\rho + e_v^z \dot{e}_v^z + \tilde{D}_\rho \dot{\tilde{D}}_\rho / \gamma_\rho + \tilde{D}_z \dot{\tilde{D}}_z / \gamma_z \\ &= e_v^\rho \left\{\dot{v}_d^\rho - \left(u_\rho + W_\rho\right)/M\right\} + e_v^z \left\{\dot{v}_d^z - \left(u_z + f_G - g + W_z\right)/M\right\} \\ &\quad + \tilde{D}_\rho \dot{\tilde{D}}_\rho / \gamma_\rho + \tilde{D}_z \dot{\tilde{D}}_z / \gamma_z.\end{aligned} \tag{19}$$

Substituting (16) into (19) gives

$$\begin{aligned}\dot{V} &= e_v^\rho \left(M\dot{v}_d^\rho - u_\rho - W_\rho\right)/M \\ &\quad + e_v^z \left(M\dot{v}_d^z - u_z - f_G + g + W_z\right)/M \\ &\quad + \tilde{D}_\rho \dot{\tilde{D}}_\rho / \gamma_\rho + \tilde{D}_z \dot{\tilde{D}}_z / \gamma_z \\ &= \frac{e_v^\rho}{M}\left\{M\dot{v}_d^\rho - \left(M\left(\dot{v}_d^\rho + k_v \tanh\left(e_v^\rho / k_v\right)\right) + \hat{D}_\rho \operatorname{sgn}\left(e_v^\rho\right)\right) - W_\rho\right\} \\ &\quad + e_v^z \left\{M\dot{v}_d^z - \left(M\left(\dot{v}_d^z + k_v \tanh\left(e_v^z / k_v\right)\right) + f_G - g\right.\right. \\ &\quad \left.\left. + \hat{D}_z \operatorname{sgn}\left(e_v^z\right)\right) - f_G + g + W_z\right\}/M + \tilde{D}_\rho \dot{\tilde{D}}_\rho / \gamma_\rho + \tilde{D}_z \dot{\tilde{D}}_z / \gamma_z \\ &\quad + \tilde{D}_\rho \dot{\tilde{D}}_\rho / \gamma_\rho + \tilde{D}_z \dot{\tilde{D}}_z / \gamma_z \\ &= -k_v e_v^\rho \tanh\left(e_v^\rho\right) - W_\rho e_v^\rho / M - \hat{D}_\rho \left|e_v^\rho\right| / M \\ &\quad - k_v e_v^z \tanh\left(e_v^z\right) - W_z e_v^z / M - \hat{D}_z \left|e_v^z\right| / M \\ &\quad + \tilde{D}_\rho \dot{\tilde{D}}_\rho / \gamma_\rho + \tilde{D}_z \dot{\tilde{D}}_z / \gamma_z \\ &\le -k_v \left\{e_v^\rho \tanh\left(e_v^\rho\right) + e_v^z \tanh\left(e_v^z\right)\right\} + D_\rho \left|e_v^\rho\right| / M - \hat{D}_\rho \left|e_v^\rho\right| / M \\ &\quad + D_\rho \left|e_v^z\right| / M - \hat{D}_z \left|e_v^z\right| / M \\ &\quad + \tilde{D}_\rho \dot{\tilde{D}}_\rho / \gamma_\rho + \tilde{D}_z \dot{\tilde{D}}_z / \gamma_z \\ &= -k_v \left\{e_v^\rho \tanh\left(e_v^\rho\right) + e_v^z \tanh\left(e_v^z\right)\right\} + \tilde{D}_\rho \left|e_v^\rho\right| / M + \tilde{D}_\rho \left|e_v^z\right| / M \\ &\quad - \tilde{D}_\rho \dot{\hat{D}}_\rho / \gamma_\rho - \tilde{D}_z \dot{D}_z / \gamma_z.\end{aligned} \tag{20}$$

If we employ the adaptive laws in (17) into (20), then

$$\dot{V} \le -k_v \left\{e_v^\rho \tanh\left(e_v^\rho\right) + e_v^z \tanh\left(e_v^z\right)\right\} \le 0. \tag{21}$$

Thus, V is bounded for all time and we have $e_v^\rho, e_v^z \in L_\infty$ and $\hat{D}_\rho, \tilde{D}_\rho, D_z, \tilde{D}_z \in L_\infty$ from (18). Also, we have $\dot{e}_v^\rho, \dot{e}_v^z \in L_\infty$ which implieds the uniform continuity of e_v^ρ and e_v^z. Combining this with L_2 property of e_v^ρ and e_v^z, we can use Barbalat's lemma (Khalil, 1992) to conclude that the tracking errors e_v^ρ and e_v^z and the estimation errors $\tilde{D}_\rho$ and $\tilde{D}_z$ converge to zero. (Q.E.D.)

Remark: As mentioned in Introduction, the proposed vector field guided auto-landing control law considers the input constraints of the airship. We have $v_d, v_d^\rho, v_d^z \in L_\infty$ from

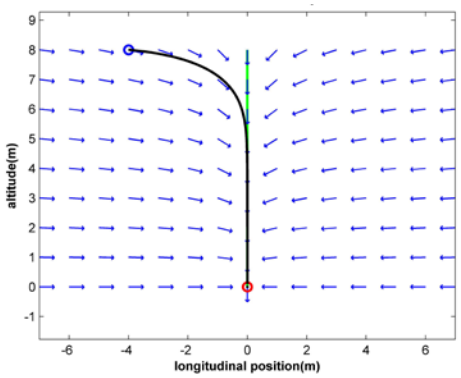

Fig. 4. The route of the airship guided by the vector field

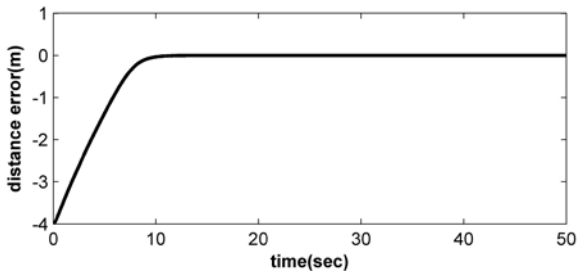

(a) The longitudinal position error

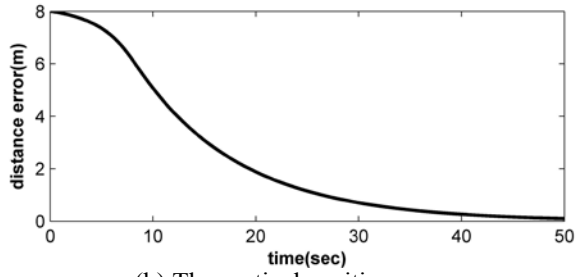

(b) The vertical position error

Fig. 5. The position errors of the airship

Theorem 1, and $\hat{\hat{D}}_\rho, D_z \in L_\infty \cap L_2$ from Theorem 2. If it can be assumed that $\dot{v}_d^\rho, \dot{v}_d^z \in L_\infty$, the control inputs, u_ρ and u_z, in (16) are bounded. Accordingly the control inputs realizing the desired course cover the input constraints of the airship.

5 SIMULATION RESULTS

In regards to the numerical simulation, we consider the airship dynamics in Fig. 1 and (1)-(4). The initial position of the airship is $\left(\rho_c(0), z_c(0)\right) = \left(-4(m), 8(m)\right)$ on the vertical plane, the initial velocities and accelerations are zero,

respectively, the initial condition of the estimates of the bounds of the wind disturbance are $\hat{D}_\rho(0) = 0$ and $\hat{D}_z(0) = 0$, the mass of the airship is $M = 4(kg)$, the force of gas in the airship is $f_G = 8$, and the disturbances are set as $W_\rho = 2$ and $W_h = 2$. Also the control gains are assigned as $k_d = 8$, $k_p = 0.2$, $k_v = 6$, $\gamma_\rho = 9$, and $\gamma_z = 8.5$. As can be seen in Fig. 4, the airship moves to the goal position while it follows the desired direction which is the direction of the vector filed. The position errors of the airship presented in

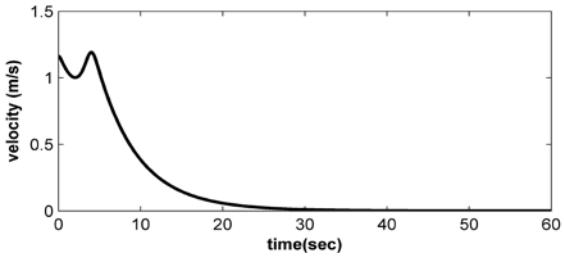

(a) The desired velocity, v_d

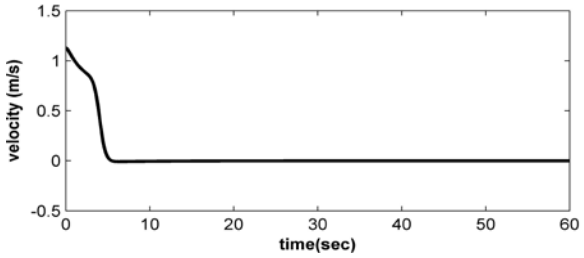

(b) The desired longitudinal velocity, v_d^ρ

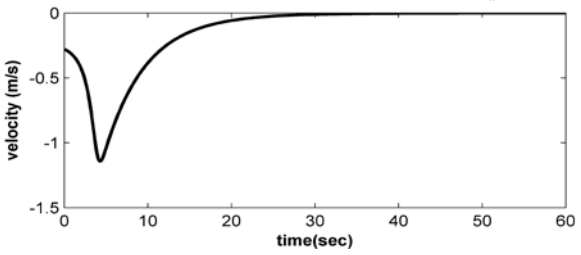

(c) The desired vertical velocity, v_d^z

Fig. 6. The desired velocities of the airship, v_d, v_d^ρ, and v_d^z.

Fig. 4 are shown in Fig. 5. In Fig. 5, we can see that the longitudinal position ρ_c and the altitude z_c converge to zero, asymptotically. The desired velocities generated using the desired course angle $\theta_d(\rho_c, z_c)$ and the desired velocity are presented in Fig. 6. Velocity errors controlled by the velocity control laws in (16) and (17) realizing the desired velocities are depicted in Fig. 7. In Fig. 7, we can sure that the velocity errors converge to zero in spite of the wind disturbances. Also, to make sure that the estimation errors converge to zero as time goes on, the estimation errors of the bounds of the wind disturbances are depicted in Fig. 8. Fig. 8 shows that the estimation errors $\tilde{D}_\rho$ and $\tilde{D}_h$ converge to zero by proposed the adaptive laws in (17). Fig. 9 shows the routes of the airships with the following initial conditions: $\left(\rho_c(0), z_c(0)\right)$=(-2, 8), (-4,4), (-6, 0), (2, 8), (4,4), and (6, 0). It can be seen in Fig. 9 that the airship with the proposed the auto-landing algorithm converges to goal position. It can be noted here that when the initial altitude of the airship is low, the airship rises because of the wind disturbance, but this unexpected motion is corrected around the goal position.

6. CONCLUSIONS

We addressed the auto-landing algorithm of the airship using the decoupled dynamics based on the vector field method. To guide the airship to the goal position, we generated the desired course using the novel vector field considering the

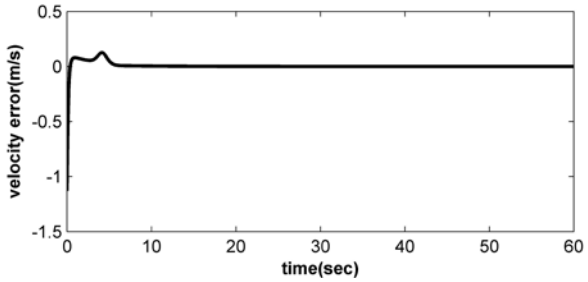

(a) The longitudinal velocity error, e_v^ρ

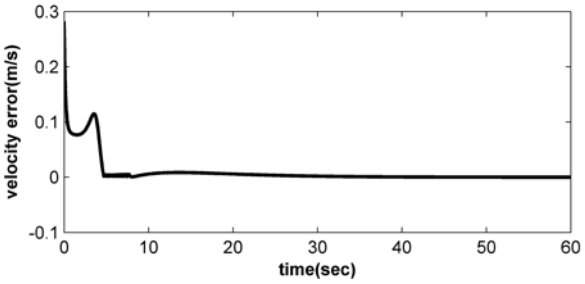

(b) The vertical velocity error, e_v^z

Fig. 7. The velocity errors, e_v^ρ and e_v^z.

ground distance and the altitude. Then, the desired velocities to let the airship follow the desired course were generated. The convergence of the velocity errors with the wind disturbances to zero was guaranteed by the proposed robust adaptive control law. In addition, the simulation results showed that the airship can move along the desired course by approaching the goal path and the desired position. As a future works, it can be followed that the model of the airship extended to three dimensional space. And the issue for the auto-landing to moving platform will be pursued by estimating the moving landing platform. Also, the proposed auto-landing algorithm will be employed to not only UAVs with the aerostatic force but also UAVs using the aerodynamic force.

ACKNOWLEDGEMENT

This research was supported by Basic Science Research Program through the National Research Foundation of Korea (NRF) funded by the Ministry of Science, ICT & Future Planning (NRF-2013R1A1A1012038) and the MSIP (Ministry of Science, ICT and Future Planning), Korea, under the "IT Consilience Creative Program" (NIPA-2014-H0201-14-1002) supervised by the NIPA (National IT Industry Promotion Agency).

REFERENCES

Azinheira, J. R. and Moutinho, A. (2008). Hover control of an UAV with backstepping design including input saturations. *IEEE Transactions on Control Systems Technology*, 16(3), 517-526.

Chwa, D. (2010). Tracking control of differential-drive wheeled mobile robots using a backstepping-like feedback linearization. *IEEE Transactions on Systems, Man, and Cybernetics-Part A: Systems and Humans*, 40(6), 1285-1295.

Kahale, E., Garcia, P. C., and Bestaoui, Y. (2013). Autonomous path tracking of a kinematic airship in presence of unknown gust. *Journal of Intelligent and Robotic Systems*, 69(1-4), 431-446.

Khalil, H. K. (1992). *Nonlinear Systems*, Macmillan Co., New York.

Kingston, D. and Beard, R., (2007) UAV splay state configuration for moving targets in wind. *LNCIS*, 396, 109-128.

Malaek, S. M. B., Sadati, N., Izadi, H., Parkmehr, M. (2004). Intelligent autolanding controller design using neural networks and fuzzy logic. *2004 5th Asian Control Conference*, Melbourne Australia.,

Moutinho, A. And Azinheira. J. R (2005). Stability and robustness analysis of the AURORA airship control system using dynamic inversion. *Proceedings of the 2005 IEEE International Conference on Robotics and Automation*, Barcelona Spain.

Pavia, E. C., Azinheira, J. R., Ramos, J. G., Moutinho, A., and Bueno, S. S. (2006). Project AURORA: infrastructure and flight control experiments for a robotic airship. *Journal of Field Robotics*, 23(3-4), 201-222.

Solaque, L, Pinzon, z., and Duque, M. (2008). Nonlinear control of the airship cruise flight phase with dynamical decoupling, E*lectronics, Robotics and Automotive Mechanics Conference, 2008,* Morelos Mexico.

Zheng, Z., Huo, W., and Wu, Z. (2012). Trajectory tracking control for underacturated stratospheric airship. *Advances in Space Research*, 50(7), 906-917.

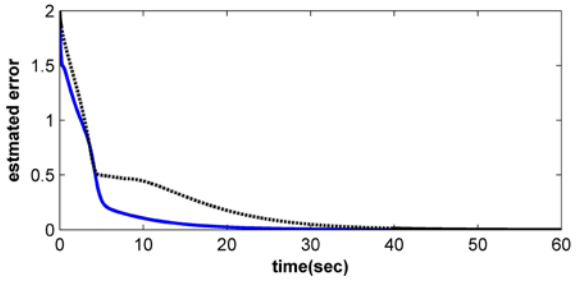

Fig. 8. The estimation errors, $\tilde{D}_\rho$ and $\tilde{D}_z$ (solid line: $\tilde{D}_\rho$, dotted line: $\tilde{D}_z$).

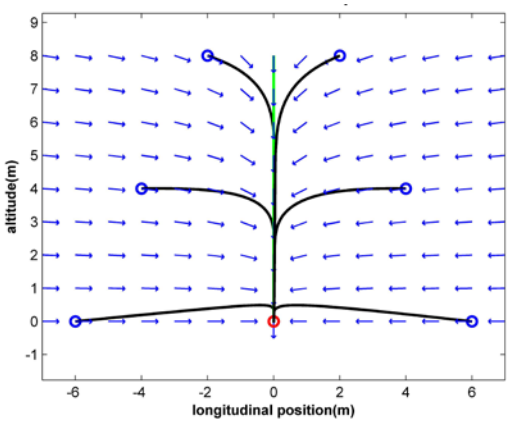

Fig. 9. The routes of the airship with respect to the various initial conditions.